Atomic Structure of the (310) Twin in Niobium: Experimental Determination and Comparison with Theoretical Predictions

Geoffrey H. Campbell,[1] Stephen M. Foiles,[2] Peter Gumbsch,[3],[a] Manfred Rühle,[3] and Wayne E. King[1]

[1]*Lawrence Livermore National Laboratory, Livermore, California 94550*
[2]*Sandia National Laboratories, Livermore, California 94551*
[3]*Max-Planck-Institute für Metallforschung, Institut für Werkstoffwissenschaft, Seestrasse 92, 7000 Stuttgart 1, Federal Republic of Germany*

(Received 21 August 1992)

The atomic structure of the (310) twin in Nb was predicted using interatomic potentials derived from the embedded atom method (EAM), Finnis-Sinclair theory (FS), and the model generalized pseudopotential theory (MGPT). The EAM and FS predicted structures with crystal translations which break mirror symmetry. The MGPT predicted one stable structure which possessed mirror symmetry. This defect was experimentally determined to have mirror symmetry. These findings emphasize that the angular dependent interactions modeled by the MGPT are important for determining defect structures in bcc transition metals.

PACS numbers: 61.16.Bg, 61.72.Mm

Atomistic simulations which can model the interactions of many tens of thousands of atoms are increasingly used as a predictive tool and have the potential to play an important role in the overall understanding of the properties of the solid state [1], such as the atomic structure of defects [2], segregation [3], and fracture [4]. The present investigation seeks experimental distinction between several models of the interatomic interactions used in these types of calculations. In particular, the interest is to assess the differences among the embedded atom method (EAM) [5,6], Finnis-Sinclair theory (FS) [7], and the model generalized pseudopotential theory (MGPT) [8] for predicting the atomic structure of defects in body-centered-cubic (bcc) transition metals and whether the predictions correspond with experimental observations. The predictive power of the EAM and FS for face-centered noble metals is well established [2,9]. Defect structures in bcc transition metals may be less easily predicted due to the partial filling of the *d* bands which is expected to add an angular dependence to the interactions [10].

The grain-boundary calculations studied here differ primarily by the absence or inclusion of angular dependent interactions. The EAM and FS potentials are both of the pair-functional form [10], where the energy contains a term which is a function of a simple pairwise sum over neighbors. They incorporate the trend that higher coordination implies longer, weaker bonds. However, they include no angular dependence of the atomic interactions. In contrast, the MGPT potentials incorporate three- and four-body interactions based on a model treatment of canonical *d* bands [8]. Only potentials which incorporate angular dependencies have been shown to predict the correct reconstruction of Mo and W (100) surfaces [11,12], while this is not possible with pair-functional methods [13]. Grain boundaries are more similar to the bulk than surfaces, possessing comparable coordination, and should provide additional information on the importance of angular dependent interactions due to the different atomic arrangements. Other potential forms which incorporate angular dependent interactions are being pursued by a number of investigators [10,14, 15], but, at present, little experimental data exist for grain-boundary structures in bcc transition metals [16,17].

High-resolution transmission electron microscopy (HREM) is a useful tool for characterizing the atomic structure of certain high symmetry grain boundaries [18,19]. Likewise, theory is limited to studying "special" grain boundaries which are periodic in the plane of the boundary. Because of these limitations, the comparison between theoretically predicted grain-boundary structures and experimentally characterized structures requires the fabrication of model grain boundaries, which was done in this study by diffusion bonding of single crystals. Diffusion bonding allows complete freedom in the selection of the orientation of a bicrystal. HREM reveals atomic structure via comparison of experimental images with images simulated using a model atomic structure as the input [20]. The comparison of simulated with experimental images then allows the choice of the model which best fits the data.

The structure of the symmetric 36.9° tilt grain boundary with [001] tilt axis forming a twin about (310) has been calculated using EAM [21], FS [22], and MGPT [23] potentials for Nb. The size of the simulation cell was chosen corresponding to the expected periodicity of the grain boundary ($\Sigma 5$ within the coincident site lattice [24] model). To explore the formation of different metastable grain-boundary structures, many different translational states of the adjacent crystals were used as initial conditions for the energy-minimization calculation.

The calculated structures for the three models are shown in Fig. 1. The MGPT potential predicts a struc-

© 1993 The American Physical Society

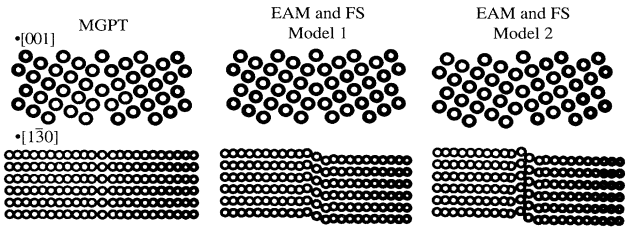

FIG. 1. Model atomic structures of the (310) twin in Nb predicted by the various interatomic potentials indicated. The model structures are shown in two orientations: The top row has a viewing direction parallel to the tilt axis of [001] while the bottom row is perpendicular to the tilt axis along [1$\bar{3}$0]. In each case, the grain boundary runs vertically.

ture which exhibits mirror symmetry across the interface and is very close to a $\Sigma 5[001]/(310)$ unrelaxed structure. Within the MGPT, this structure was the only one found to be stable. As expected from the similarity of the methods, the use of the EAM and FS potentials led to nearly identical results. They predicted several metastable structures. The two shown in Fig. 1 ("model 1" and "model 2") exhibited the lowest energies. There exist translational shifts between the adjacent crystals which differentiate model 1 and model 2 from the MGPT prediction. In model 1 there is a relative shift in the crystal positions by a translation of 0.078 nm in the [001] direction, corresponding to half a (002) lattice plane spacing. Model 2 includes a crystal translation of 0.083 nm in the [001] direction as well as a translation of 0.052 nm in the [1$\bar{3}$0] direction in the plane of the boundary. The mirror symmetric structure predicted by the MGPT is stable when simulated using EAM potentials, but the energy of the structure, 1.20 J/m^2, is significantly greater than that of the two other structures, 1.03 J/m^2 for model 1 and 0.98 J/m^2 for model 2. Additionally, when model 1 and model 2 are used as the initial configurations for the MGPT calculation, they are unstable and relax to the MGPT structure shown. One of the effects of the angular terms in the MGPT is to penalize structures containing right angles and to favor those with angles around 71° [10], which is the nearest-neighbor bond angle in the bcc structure. Model 2 contains a significant number of right angles at the boundary, whereas the other two models do not.

Grain boundaries forming (310) twins in Nb were prepared by diffusion bonding two precisely oriented, to within $\pm 0.1°$, Nb single crystals with flat polished (310) surfaces which were misoriented by 180° about [310] relative to the perfect crystal [25]. Two projections are required for a complete HREM investigation. For this case [001] and [1$\bar{3}$0], which lie in the interface, were chosen. Image simulation [26] was performed using the multislice formalism [27]; for details see [28,29].

A high-resolution micrograph is shown in Fig. 2. Both crystals are viewed in the [001] direction. Crystallographically flat, straight sections of the boundary on

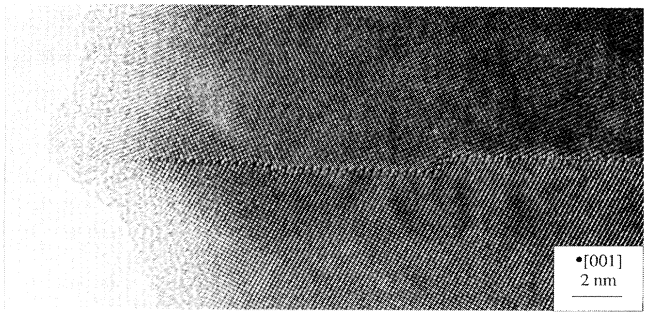

FIG. 2. A high-resolution image of the (310) twin in Nb viewed along [001]. The grain boundary runs horizontally. Straight, flat sections of the boundary indicate faceting. The facets provide atomically perfect regions of the (310) twin for study.

(310) planes (for both crystals) are seen to be separated by small regions of severe mismatch.

Image simulations based on the models in Fig. 1 for the viewing direction parallel to the tilt axis are shown in Fig. 3. There is essentially no difference between the simulated image from the MGPT and model 1. The simulated intensities differ by less than 1% for all values of thickness and defocus investigated. The crystal shift parallel to the tilt axis is indiscernible when viewed along [001]. But when there is a shift in the [1$\bar{3}$0] direction, as in model 2, different contrast at and near the boundary can be observed. The comparison of the simulated image using the MGPT (or model 1) to the experimental image is shown in Fig. 4. Comparison of the spot patterns makes it clear that a match to the simulation using model 2 can be ruled out. This result was confirmed by also comparing experimental and simulated images for other focus values [29].

The [1$\bar{3}$0] direction, orthogonal to the first viewing direction, is most suitable for the second projection of the grain-boundary structure. The largest spaced atomic planes of Nb parallel to [1$\bar{3}$0] are (002) and (310), with interplanar spacings of 0.165 and 0.104 nm, respectively. The spacing of the (310) is below the information limit of the microscope, which is approximately 0.14 nm. The (002) reflections will be the only ones contributing to the

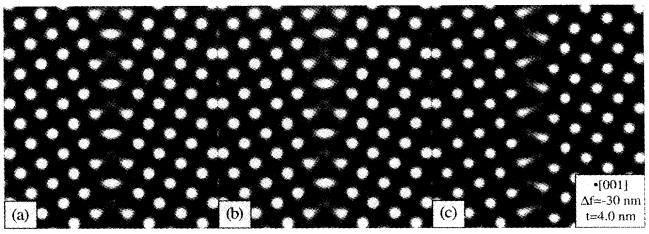

FIG. 3. Simulated high-resolution images using the model (310) twin structures as viewed along [001]: (a) MGPT, (b) EAM and FS model 1, and (c) EAM and FS model 2. The focus deviation from Gaussian, Δf, and the crystal thickness, t, are shown.

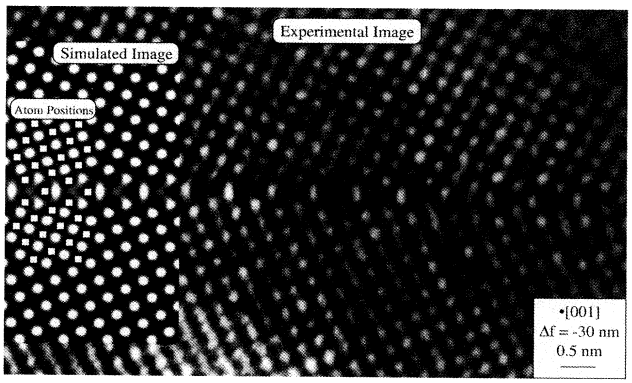

FIG. 4. Comparison of experimental image with simulated image. The simulated image uses the MGPT model atomic structure from Fig. 1, but the result would be identical if EAM and FS model 1 were used. The positions of the atomic columns are indicated by white boxes.

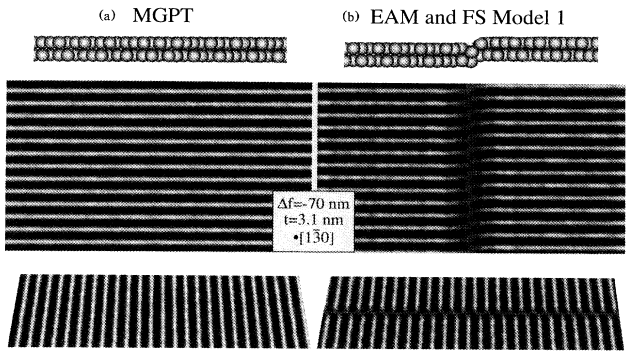

FIG. 5. Simulated high-resolution images using the remaining model (310) twin structures as viewed along [1$\bar{3}$0] for (a) MGPT and (b) EAM and FS model 1. The lattice fringe image arises from (002) planes with spacing of 0.165 nm. The bottom row of images are glancing-angle, perspective views of the same images as in the row above, rotated by 90° to emphasize the displacement of the lattice fringes at the boundary for model 1.

phase contrast image resulting in a lattice fringe image (Fig. 5). The (002) planes are perpendicular to the (310) twin plane and a relative shift of the adjacent crystals in [001] (model 1 and model 2) should result in a discontinuity of the (002) lattice fringes at the interface (Fig. 5). Conversely, for the MGPT model, where no shift exists between the crystals, the (002) fringes are continuous across the interface. The experimental high-resolution image corresponding to this viewing direction is shown in Fig. 6. The (002) fringes run vertically and are seen, especially easily in the glancing-angle perspective view, to be continuous across the grain boundary. Thus, the results of the high-resolution microscopy indicate that the boundary atomic structure is mirror symmetric, which agrees with the prediction of the MGPT.

One limitation for all HREM studies is that the area of grain boundary probed is very small. For example, the area imaged in Fig. 4 is approximately 3 nm thick and 5 nm long. This sampling cannot rule out the possibility of grain-boundary structural multiplicity [30]. But the extensive faceting to the (310) plane at the diffusion bonding process temperature of 1500°C indicates that the observed structure is of a relatively low energy compared to boundaries with small deviations in tilt angle from the exact $\Sigma 5$ (310) geometry. The faceting also suggests that the two high-resolution images shown, although not from the same sample, came from boundaries having the same structure.

The success of the MGPT in predicting the atomic structure of the (310) twin in Nb is due to the incorporation of multibody interactions in the model. Partial filling of the *d* bands in Nb imparts a directionality to the bonding, suggesting that these bond-angle effects may also be important for other central transition metals. The similar results obtained by the EAM and FS potentials indicate that their failure results from an inadequacy of pair-functional methods rather than from possible problems associated with the practical implementation of these potentials. Grain-boundary structures in bcc metals have also been studied using pair potentials designed to model Fe and simple metals [31]. Symmetric boundaries were found despite the lack of angularly dependent interactions. The metals for which these potentials were designed are not expected to have large bond-angle effects; thus the pair-potential treatment is better justified. The current results indicate that the pair-functional potentials of the type used here are inadequate for Nb. Although the repulsive part of the MGPT potential appears too stiff [28], such potentials incorporating angularly dependent interactions will be required for Nb and probably the other central transition metals where direc-

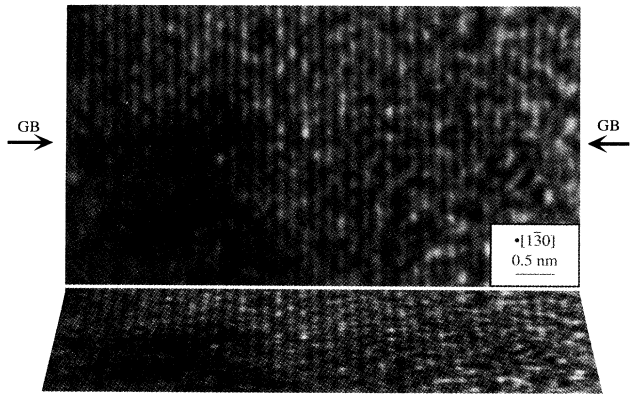

FIG. 6. A high-resolution image of the (310) twin in Nb as viewed along [1$\bar{3}$0]. The boundary runs horizontally between the arrows. At bottom is a glancing-angle, perspective view of the image to emphasize that the (200) lattice fringes run straight across the boundary without any displacements due to relative shifts of the crystals.

tional bonding due to partially filled d bands is important.

This work was performed under the auspices of the Division of Materials Science of the Office of Basic Energy Sciences, U.S. DOE, and LLNL under Contract No. W-7405-Eng-48. Part of this work was performed while G. H. Campbell was at the MPI f. Metallforschung, Stuttgart, and was supported by the Alexander von Humboldt Foundation. We would like to thank W. Wien for his careful preparation of the Nb crystals, D. Korn for his assistance with the UHV diffusion bonding machine, and Dr. J. A. Moriarty for providing the MGPT potential for Nb prior to publication.

[a]Present address: Department of Mathematics, Imperial College, 180 Queens Gate, London SW7 2BZ, United Kingdom.

[1] *Atomistic Simulation of Materials*, edited by V. Vitek and D. J. Srolovitz (Plenum, New York, 1989).

[2] M. I. Baskes, S. M. Foiles, and M. S. Daw, Mater. Sci. Forum **46**, 187 (1989).

[3] S. M. Foiles, in *Surface Segregation Phenomena*, edited by P. A. Dowben and A. Miller (CRC, Boca Raton, FL, 1990), p. 79.

[4] S. Kohlhoff, P. Gumbsch, and H. F. Fischmeister, Philos. Mag. A **64**, 851 (1991).

[5] M. S. Daw and M. I. Baskes, Phys. Rev. Lett. **50**, 1285 (1983).

[6] M. S. Daw and M. I. Baskes, Phys. Rev. B **29**, 6443 (1984).

[7] M. W. Finnis and J. E. Sinclair, Philos. Mag. A **50**, 45 (1984).

[8] J. A. Moriarty, Phys. Rev. B **42**, 1609 (1990).

[9] U. Dahmen *et al.*, Philos. Mag. Lett. **62**, 327 (1990).

[10] A. E. Carlsson, in *Advances in Research and Applications*, edited by H. Ehrenreich and D. Turnbull, Solid State Physics Vol. 43 (Academic, New York, 1990), p. 1.

[11] J. A. Moriarty and R. B. Phillips, Phys. Rev. Lett. **66**, 3036 (1991).

[12] A. E. Carlsson, Phys. Rev. B **44**, 6590 (1991).

[13] G. J. Ackland and M. W. Finnis, Philos. Mag. A **54**, 301 (1986).

[14] D. G. Pettifor, Phys. Rev. Lett. **63**, 2480 (1989).

[15] M. I. Baskes, Phys. Rev. B **46**, 2727 (1992).

[16] J. M. Pénisson, R. Gronsky, and J. B. Brosse, Scr. Metall. **16**, 1239 (1982).

[17] J. M. Pénisson, T. Nowicki, and M. Biscondi, Philos. Mag. A **58**, 947 (1988).

[18] K. L. Merkle and D. Wolf, Bull. Mater. Res. Soc. **15**, 42 (1990).

[19] P. Pirouz and F. Ernst, in *Metal-Ceramic Interfaces*, edited by M. Rühle, A. G. Evans, J. P. Hirth, and M. F. Ashby (Pergamon, New York, 1990), p. 199.

[20] J. C. Barry, in *Computer Simulations of Electron Microscope Diffraction and Images*, edited by W. Krakow and M. O'Keefe (The Minerals, Metals, and Materials Society, Warrendale, 1989), p. 57.

[21] R. A. Johnson and D. J. Oh, J. Mater. Res. **4**, 1195 (1989).

[22] G. J. Ackland and R. Thetford, Philos. Mag. A **56**, 15 (1987).

[23] J. A. Moriarty, in *Many-Atom Interactions in Solids*, edited by R. N. Nieminen, M. J. Puska, and M. J. Manninen (Springer-Verlag, Berlin, 1990), p. 158.

[24] W. Bollmann, *Crystal Defects and Crystalline Interfaces* (Springer-Verlag, Berlin, 1970).

[25] W. E. King *et al.*, in *Defects in Materials*, edited by P. D. Bristowe, J. E. Epperson, J. E. Griffith, and Z. Liliental-Weber, MRS Symposia Proceedings No. 209 (Materials Research Society, Pittsburgh, 1991), p. 39.

[26] P. A. Stadelmann, Ultramicroscopy **21**, 131 (1987).

[27] J. M. Cowley and A. F. Moodie, Acta Crytallogr. **10**, 609 (1957).

[28] G. H. Campbell *et al.*, in *Structure/Property Relationships for Metal/Metal Interfaces*, edited by A. D. Romig, Jr., D. E. Fowler, and P. D. Bristowe, MRS Symposia Proceedings No. 229 (Materials Research Society, Pittsburgh, PA, 1991), p. 191.

[29] G. H. Campbell *et al.*, in *Structure and Properties of Interfaces in Materials*, edited by W. A. T. Clark, U. Dahmen, and C. L. Briant, MRS Symposia Proceedings No. 238 (Materials Research Society, Pittsburgh, 1992), p. 163.

[30] K. L. Merkle and D. J. Smith, Phys. Rev. Lett. **59**, 2887 (1987).

[31] V. Vitek, D. A. Smith, and R. C. Pond, Philos. Mag. A **41**, 649 (1980).

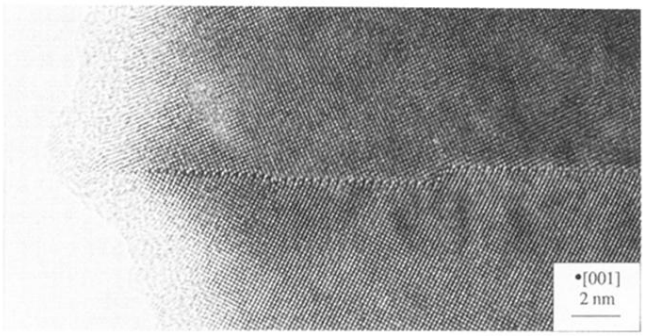

FIG. 2. A high-resolution image of the (310) twin in Nb viewed along [001]. The grain boundary runs horizontally. Straight, flat sections of the boundary indicate faceting. The facets provide atomically perfect regions of the (310) twin for study.

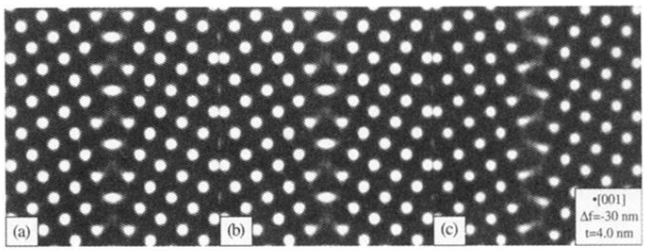

FIG. 3. Simulated high-resolution images using the model (310) twin structures as viewed along [001]: (a) MGPT, (b) EAM and FS model 1, and (c) EAM and FS model 2. The focus deviation from Gaussian, Δf, and the crystal thickness, t, are shown.

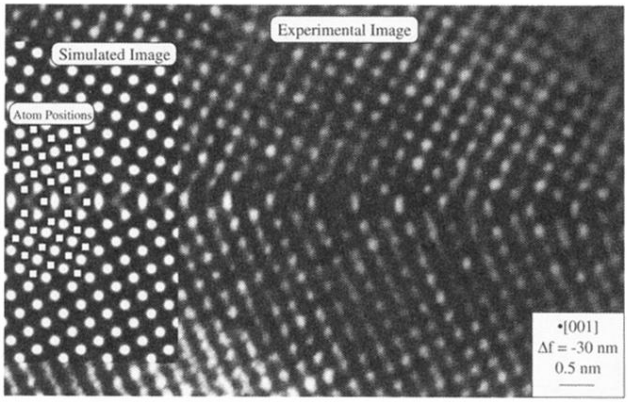

FIG. 4. Comparison of experimental image with simulated image. The simulated image uses the MGPT model atomic structure from Fig. 1, but the result would be identical if EAM and FS model 1 were used. The positions of the atomic columns are indicated by white boxes.

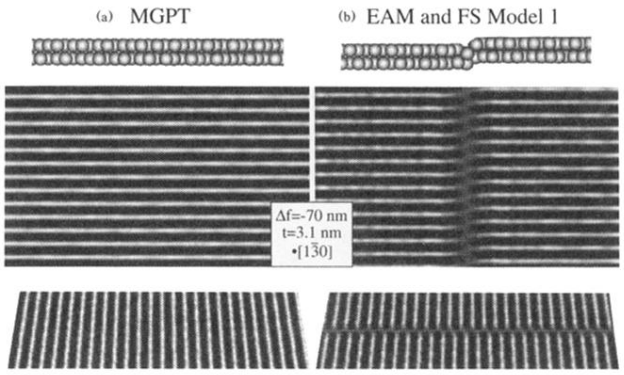

FIG. 5. Simulated high-resolution images using the remaining model (310) twin structures as viewed along [1$\bar{3}$0] for (a) MGPT and (b) EAM and FS model 1. The lattice fringe image arises from (002) planes with spacing of 0.165 nm. The bottom row of images are glancing-angle, perspective views of the same images as in the row above, rotated by 90° to emphasize the displacement of the lattice fringes at the boundary for model 1.

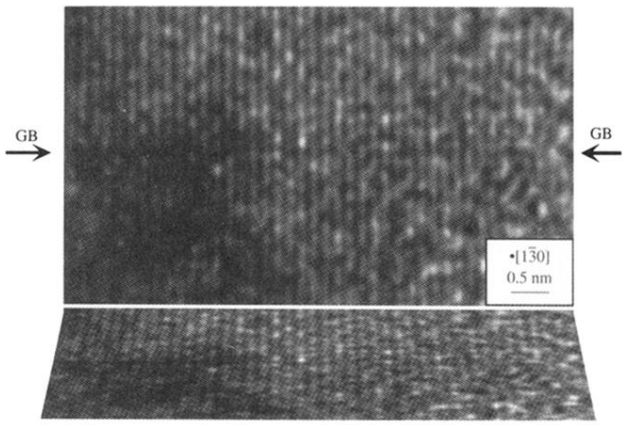

FIG. 6. A high-resolution image of the (310) twin in Nb as viewed along [1$\bar{3}$0]. The boundary runs horizontally between the arrows. At bottom is a glancing-angle, perspective view of the image to emphasize that the (200) lattice fringes run straight across the boundary without any displacements due to relative shifts of the crystals.